School of Chemical and Process Engineering

FACULTY OF ENGINEERING

UNIVERSITY OF LEEDS

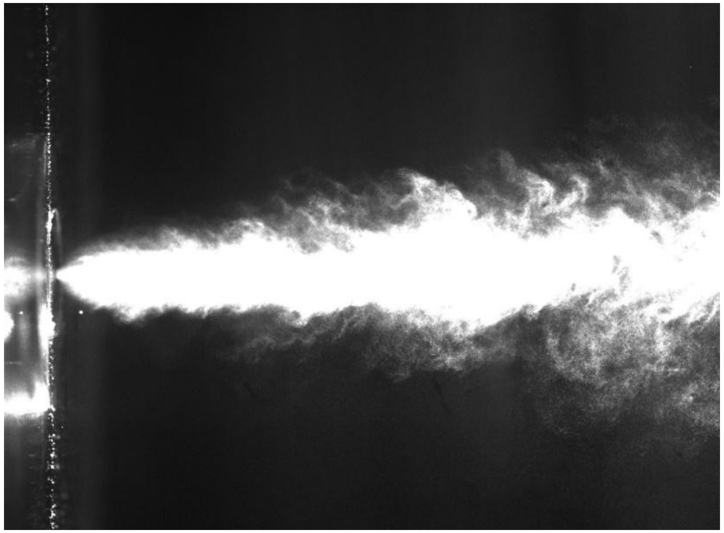

Modelling particle evolution in turbulent high pressure sonic CO_2 jets

C.J. Wareing[1,2], M. Fairweather[1], R.M. Woolley[1] and S.A.E.G. Falle[3]

[1] School of Chemical and Process Engineering,
[2]School of Physics and Astronomy,
[3]School of Mathematics,

University of Leeds, Leeds LS2 9JT, UK

8th International Symposium on Turbulence, Heat and Mass Transfer, Sarajevo, Bosnia and Herzegovina, 15th-18th September 2015

Background

- Predicting the correct turbulent fluid and solid particle behaviour during the discharge process from high pressure reservoirs of liquid carbon dioxide (CO_2) is of particular importance in several industries
- As a rapid expansion of a supercritical solution (RESS) in, for example, gas anti-solvent processes and the cleaning industry, this enables the production of fine pharmaceutical particles and jet blasting of residue from materials in situations ranging from *public highways* to *concrete walls in nuclear power stations*
- With development and roll-out of *carbon capture and storage*, pipeline transport of CO_2 is essential in order to access on- and off-shore storage sites
- Such pipelines will pass near populated areas, hence validated numerical models are required to predict behaviour of accidental releases in terms of phase composition and dispersion
- Models are subsequently used in risk assessments for planning, construction and operation of CO_2 pipelines

Outline

UNIVERSITY OF LEEDS

- Presentation describes mathematical modelling and experimental work aimed at providing validated tools for prediction of multi-phase discharges, capable of reproducing near-field fluid dynamic, phase and particle behaviour of CO_2 releases

- Focus is on modelling fluid and particle coupling in order to explain experimentally observed properties and behaviours

- Predictions of value in optimising industrial RESS cleaning processes and ensuring the safe deployment of CCS transport pipelines

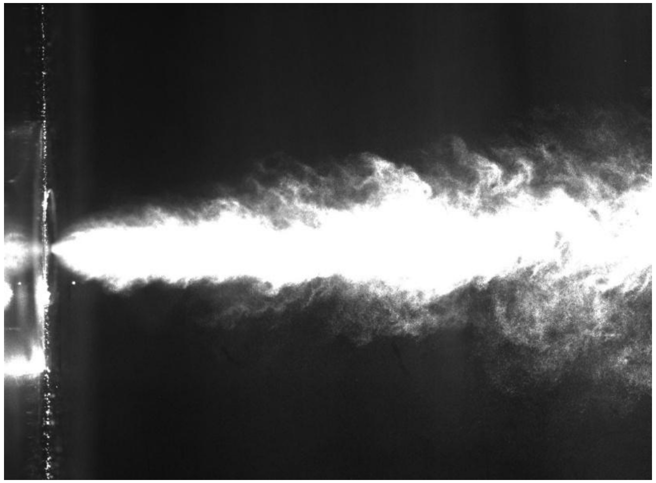

Contents

1. Experimental Measurements

Problem: where do the particles go in such a sonic CO_2 discharge?

No clear information available.

1. Experimental Measurements

UNIVERSITY OF LEEDS

Problem: where do the particles go in such a sonic CO_2 discharge?

No clear information available.

- **Solution:** Laboratory-scale experiments in a ventilated chamber
  - 20ml canister of liquid CO_2 pressurised to 68.9 bar at ambient temp
  - Connected to a nozzle at one end of a Perspex box 50x50x500mm
  - Two nozzles flush with inside of box: 0.5mm and 1.0mm in diameter (D)
  - Phase Doppler Particle Anemometry used to measure particle sizes and velocities along the sonic release
  - Data obtained at 3D, 5D, 6D, 10D, 20D, 30D, 50D and 100D
  - Experiment mimics a pipeline discharge
  - High speed video

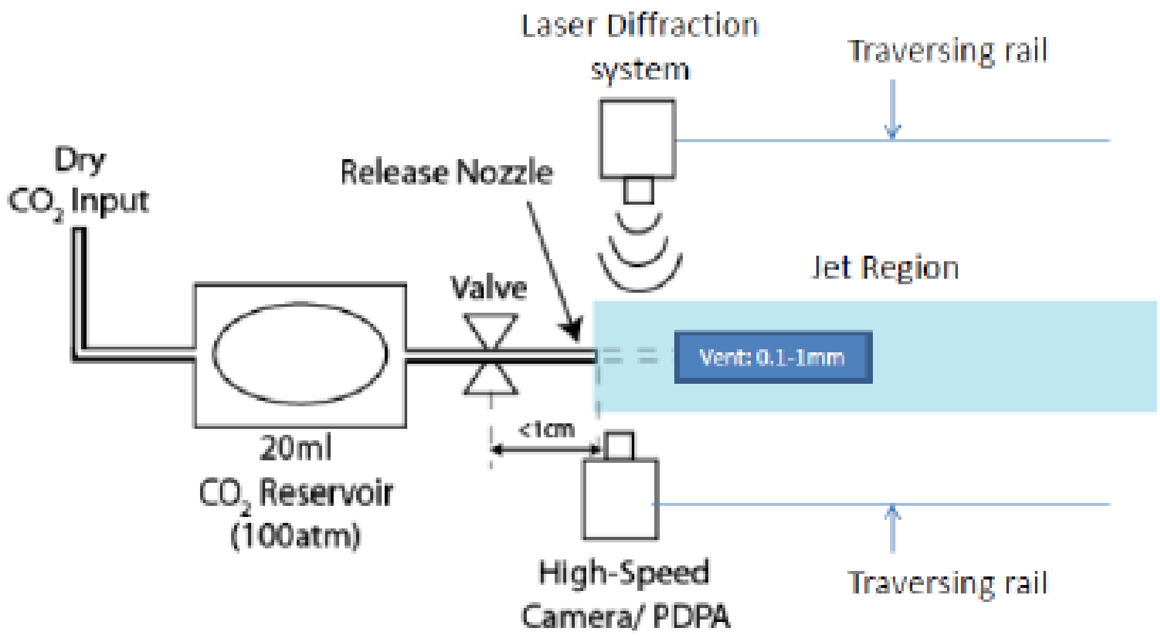

1. Experimental Measurements

UNIVERSITY OF LEEDS

A high-speed camera movie of a high pressure CO_2 release into a dry atmosphere.

Individual particles are visible.

1. Experimental Measurements

UNIVERSITY OF LEEDS

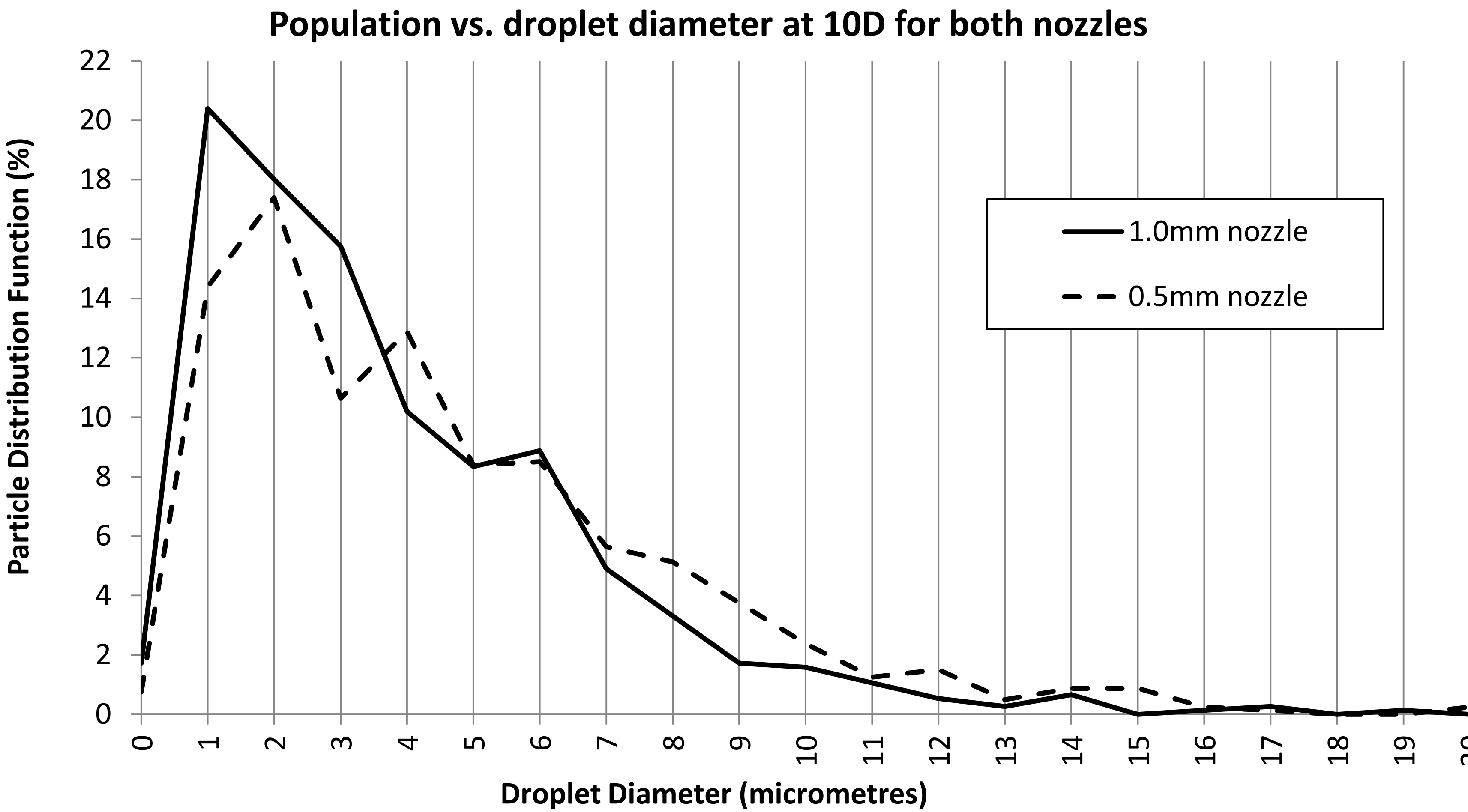

- Initial particle distribution post-Mach shock is centred on 1-2 micrometres
- These particle sizes are in agreement with Weber number predictions

1. Experimental Measurements

UNIVERSITY OF LEEDS

- 0.5mm nozzle: no agglomeration

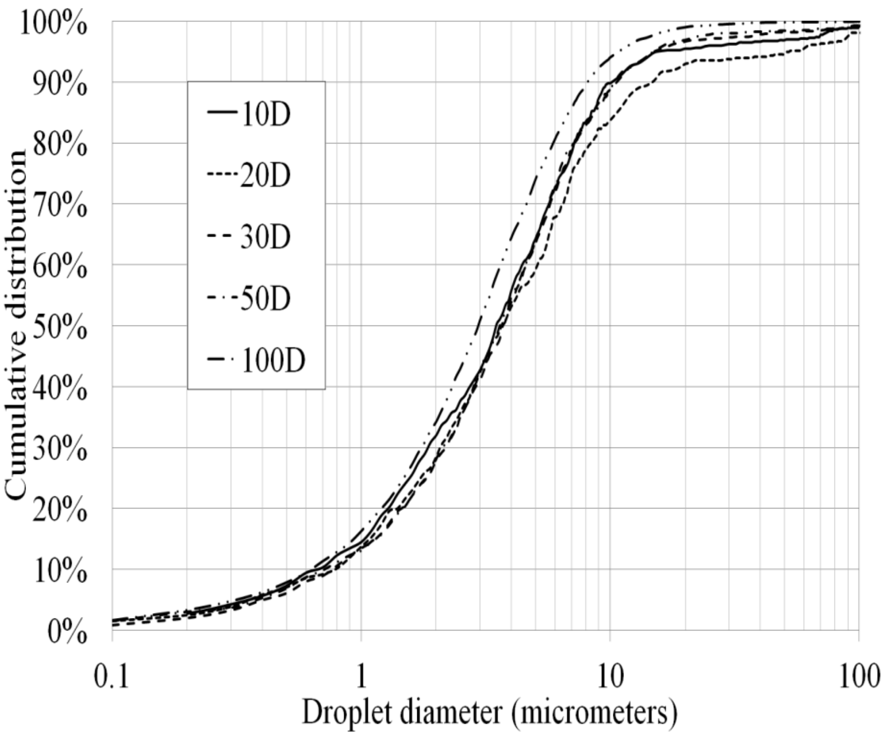

- 1.0mm nozzle: agglomeration!

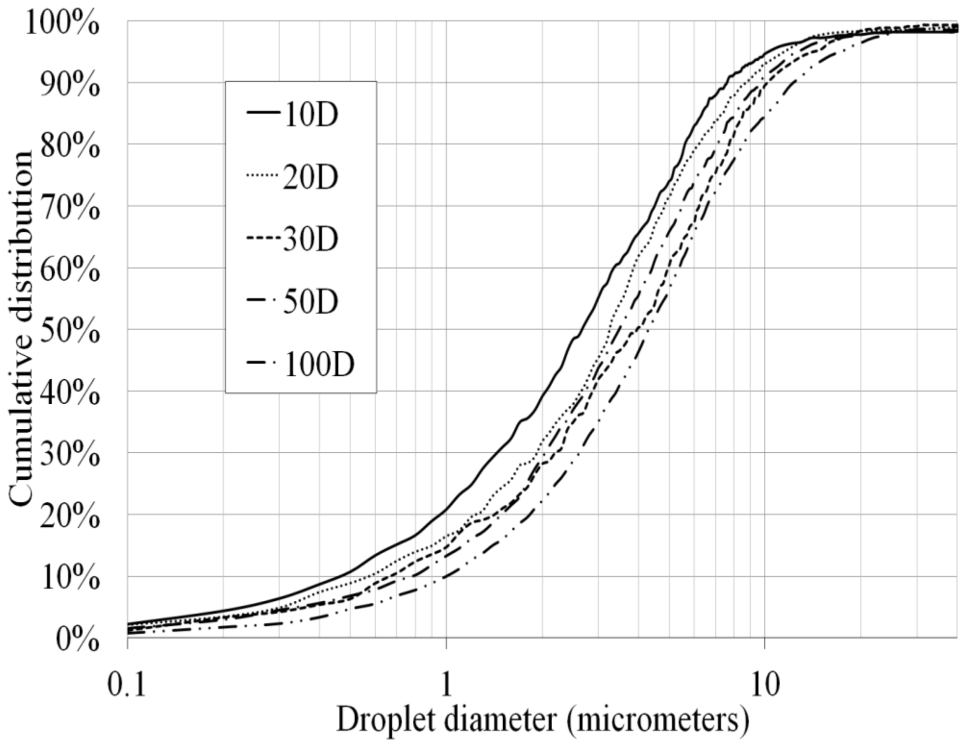

- No change in PDF along the jet for the 0.5mm nozzle case
- Shift of PDF -> evidence of agglomeration in 1.0mm nozzle case

1. Experimental Measurements

UNIVERSITY OF LEEDS

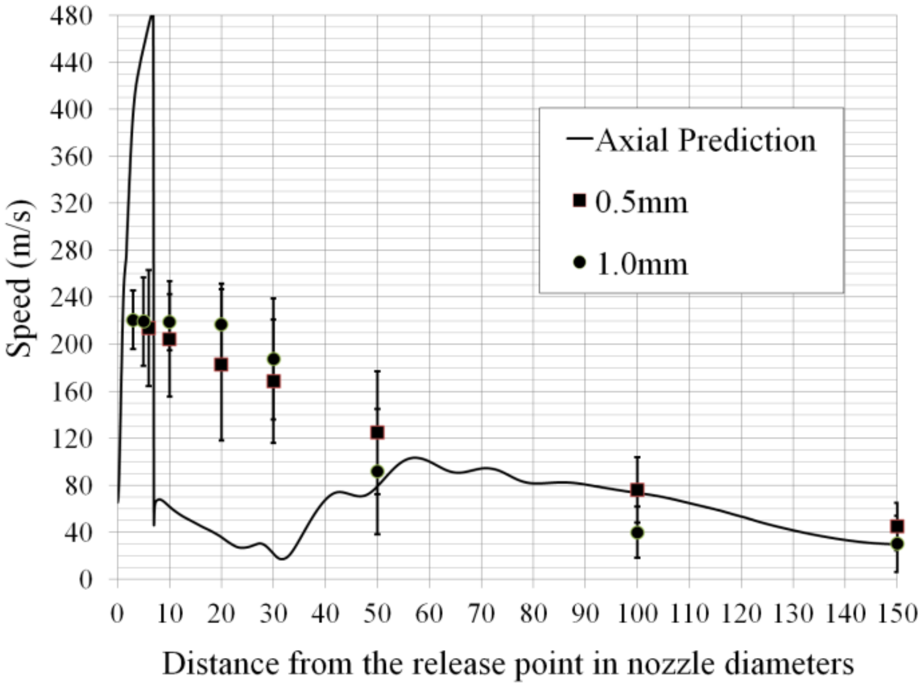

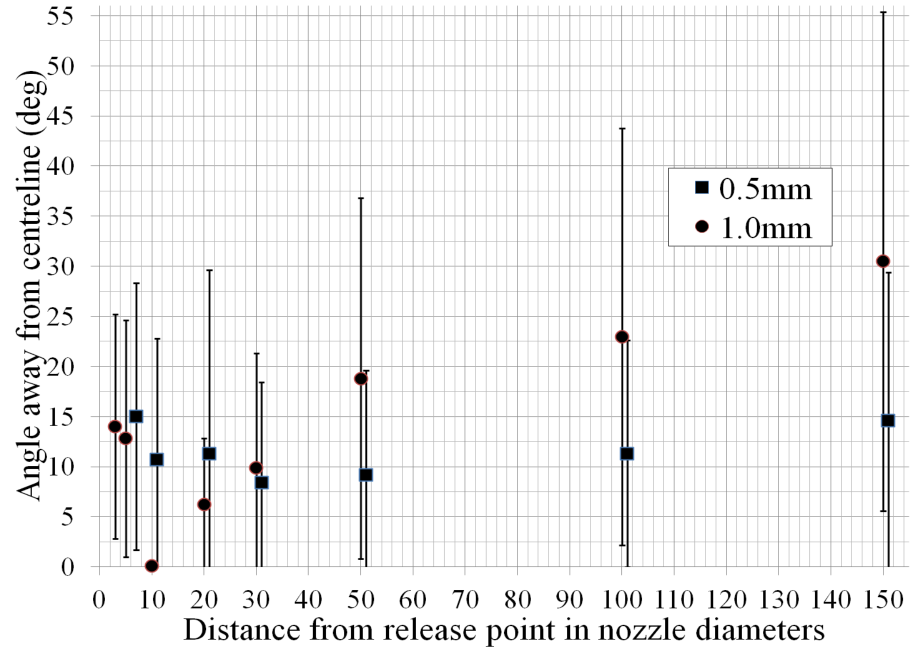

- Particles are not in equilibrium with the flow until at least 50D
- Supported by theoretical calculations of thermal and dynamic relaxation times for these specific nozzles
- Instantaneous velocities are further away from the centreline in the 1.0mm case. Indications of particles following the turbulent motion?

2. Free Release Model

UNIVERSITY OF LEEDS

Reynolds-averaged, density-weighted forms of transport equations for:

- Mass
- Momentum
- Conserved scalars (CO_2 mass fraction and CO_2 dense phase fraction)
- Total energy per unit volume (internal energy plus kinetic energy)
- Turbulence kinetic energy
- Turbulence kinetic energy dissipation rate

S = entropy per unit mass

$$\frac{\partial \bar{\rho}}{\partial t} + \frac{\partial}{\partial x_i}(\bar{\rho}\tilde{u}_i) = 0$$

$$\frac{\partial}{\partial t}(\bar{\rho}\tilde{u}_i) + \frac{\partial}{\partial x_j}(\bar{\rho}\tilde{u}_i\tilde{u}_j + \bar{p} - \bar{\rho}\widetilde{u_i''u_j''}) - s_u = 0$$

$$\frac{\partial}{\partial t}(\bar{\rho}\tilde{\beta}) + \frac{\partial}{\partial x_i}(\bar{\rho}\tilde{\beta}\tilde{u}_i) - \frac{\partial}{\partial x_i}\left[\mu_t \frac{\partial \tilde{\beta}}{\partial x_j}\right] = 0$$

$$\frac{\partial}{\partial t}(\bar{\rho}\tilde{\alpha}) + \frac{\partial}{\partial x_i}(\bar{\rho}\tilde{\alpha}\tilde{u}_i) - \frac{\partial}{\partial x_i}\left[\mu_t \frac{\partial \tilde{\alpha}}{\partial x_j}\right] - s_\alpha = 0$$

$$\frac{\partial \tilde{E}}{\partial t} + \frac{\partial}{\partial x_i}\left[(\tilde{E} + \bar{p})\tilde{u}_i - \tilde{u}_i\widetilde{u_i''u_j''}\right] - \frac{\partial}{\partial x_i}\left(\mu_t T \frac{\partial S}{\partial x_i}\right) - s_E = 0$$

$$\frac{\partial}{\partial t}(\bar{\rho}k) + \frac{\partial}{\partial x_i}(\bar{\rho}k\tilde{u}_i) - \frac{\partial}{\partial x_i}\left[\mu_t \frac{\partial k}{\partial x_i}\right] - s_k = 0$$

$$\frac{\partial}{\partial t}(\bar{\rho}\varepsilon) + \frac{\partial}{\partial x_i}(\bar{\rho}\varepsilon\tilde{u}_i) - \frac{\partial}{\partial x_i}\left[\mu_\varepsilon \frac{\partial \varepsilon}{\partial x_i}\right] - s_\varepsilon = 0$$

3. Numerical Method

- Adaptive, finite-volume grid algorithm with rectangular mesh
- Grid adaption achieved by successive overlaying of refined layers of computational mesh
  - For steep gradients in variables, e.g. at Mach shock, mesh more refined. Generation of fine grids in regions of high spatial and temporal variation
  - Conversely, coarser grids allowed where flow field is smooth
- k-ε turbulence model available, including compressibility correction according to Sarkar et al (1991)
- Second-moment Reynolds stress turbulence model available, including round-jet correction according to Dianat et al (1996)
- Solutions obtained for time-dependent, density-weighted equations
- Efficient, general-purpose shock-capturing, upwind, second-order-accurate Godunov numerical scheme with Harten, Lax, van Leer Riemann solver

3. Adaptive Mesh Method

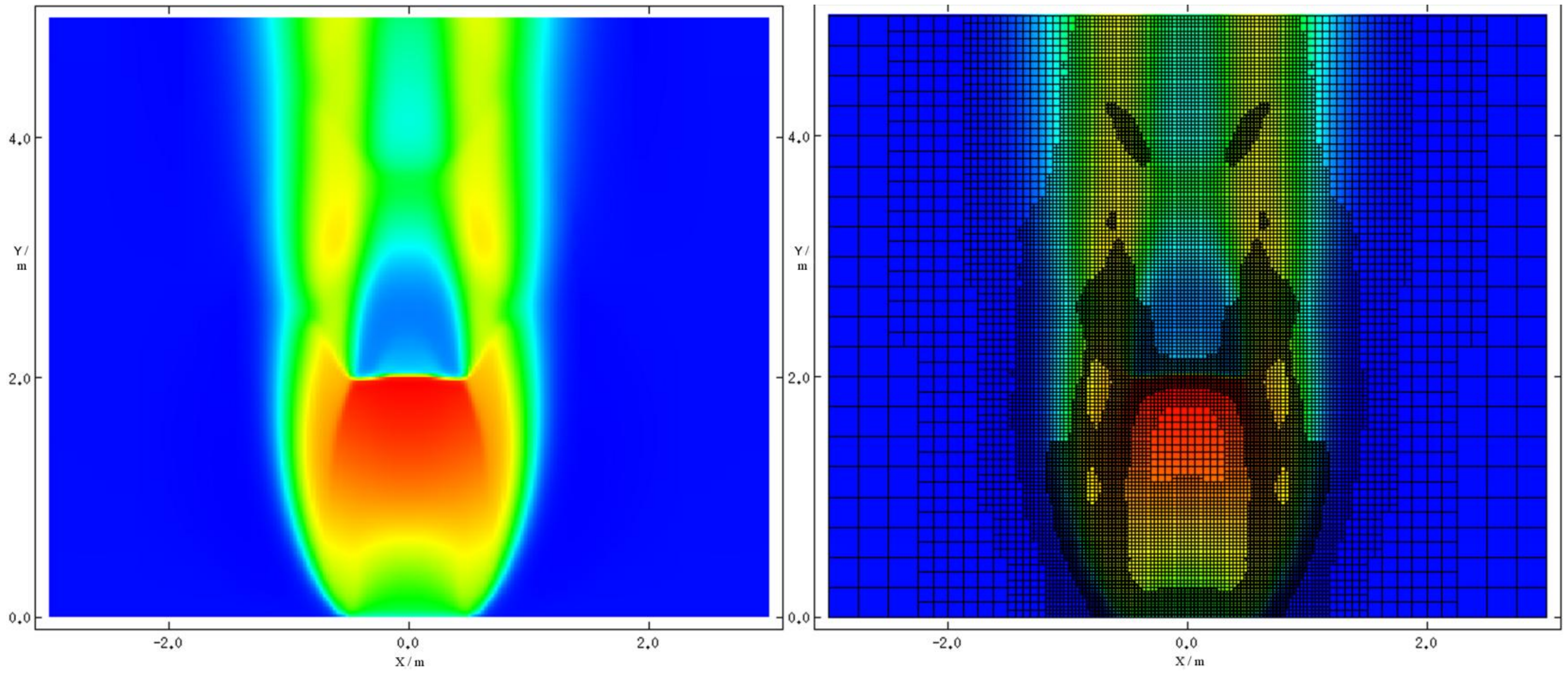

Adaptive mesh refinement grid mapped onto mean velocity predictions in the region of a Mach disc

4. Thermodynamic Model

- Novel composite equation of state for pure CO_2 employing:
  - Peng-Robinson (1976) equation of state in gas phase
  - Tabulated data derived from Span and Wagner (1996) equation of state for liquid phase and vapour pressure
  - Improved Jager and Span (2012) equation of state for solid CO_2
- Calculations undertaken using Helmholtz free energy in terms of temperature and molar volume, as all other thermodynamic properties can be readily obtained from it

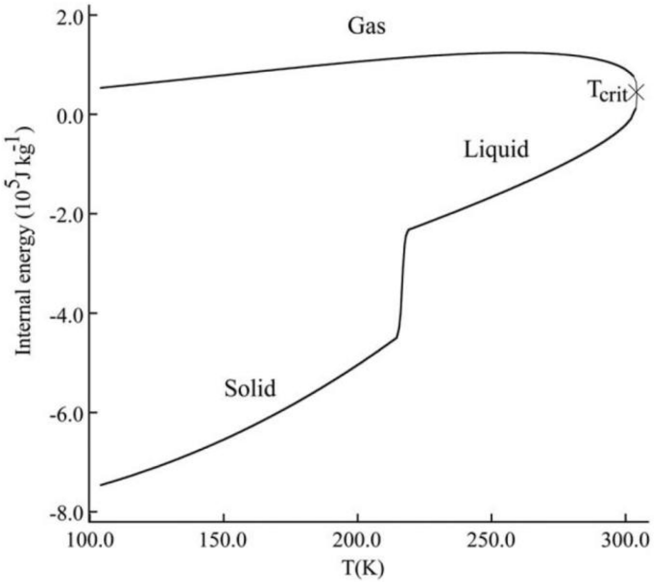

- Internal energy on saturation line
- T_{crit} marks critical temperature
- Triple point can be identified by steep connection between liquid and solid phases – latent heat of fusion

5. Validation – dense phase free release

UNIVERSITY OF LEEDS

Measuring planes at:

- 4m (165D)
- 7m (288D)

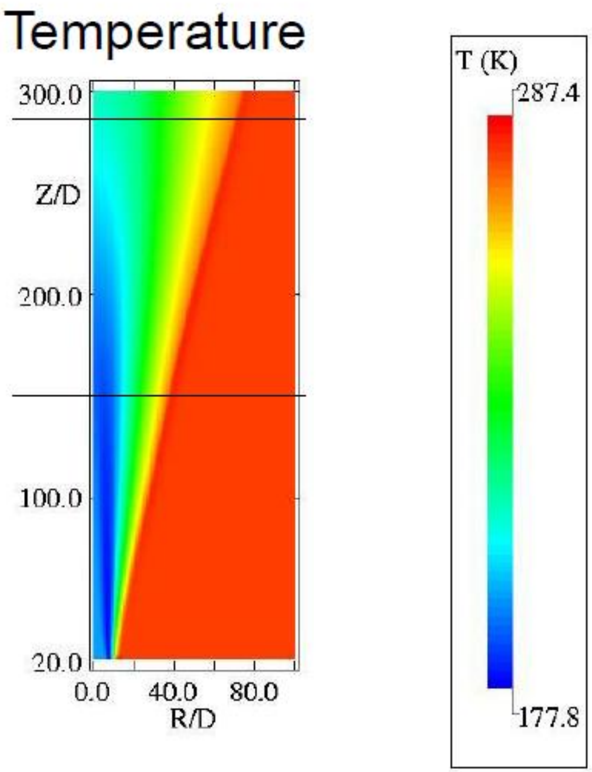

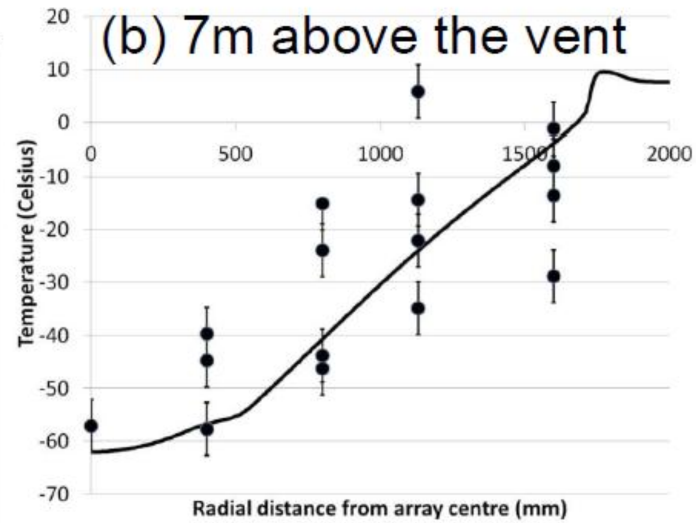

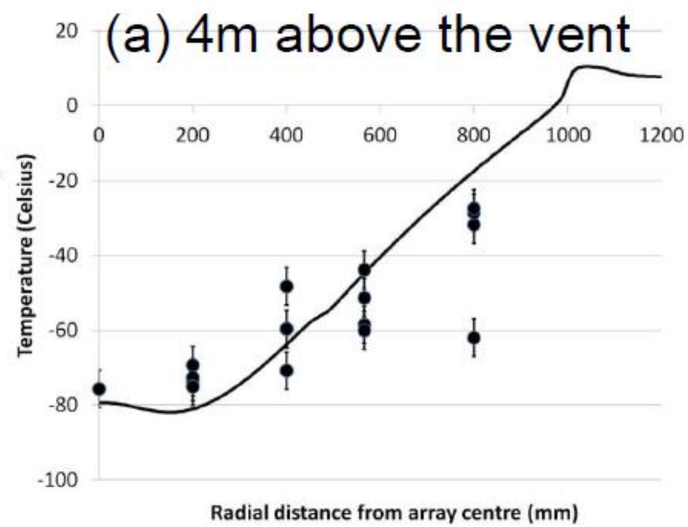

Predictions

- Core temperatures good.
- Jet widths good.
- Some cross-wind effects.

5. Validation – multiple datasets

UNIVERSITY OF LEEDS

• A comparison between experimental data and numerical prediction along the centreline of the jet and radially at 165D and 400D along the centreline.

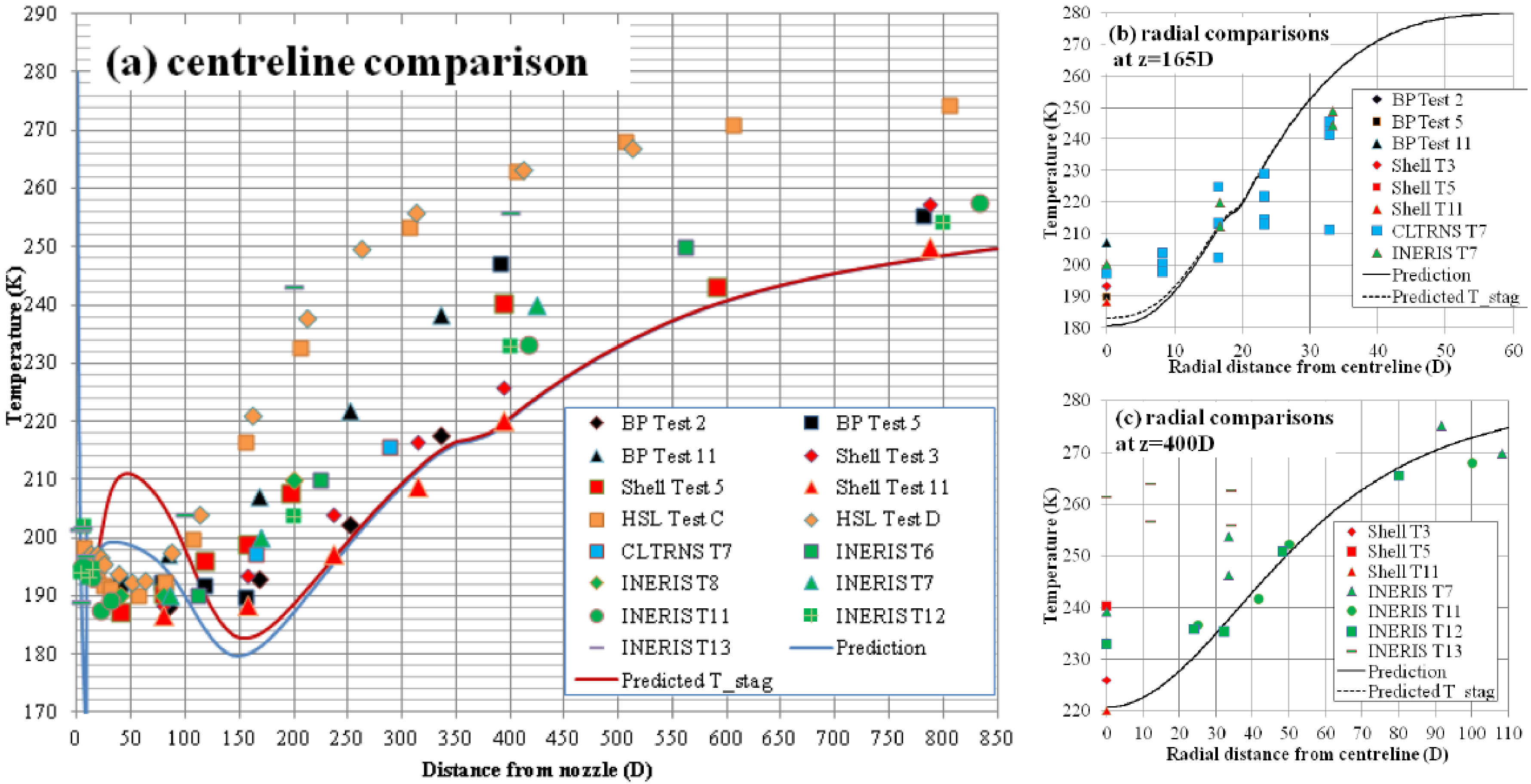

• Experimental errors of ±5K throughout; error bars omitted for clarity.

6. Particle Evolution Model

UNIVERSITY OF LEEDS

- Motion of particles computed using Lagrangian particle tracker
- Viscous drag in the low Reynolds number regime included
- Turbulent shear agglomeration model dependent on $\sqrt{\varepsilon}$
    - Reproduces observed agglomeration in the 1.0mm diameter case
- Particle mass changes according to

$$\frac{1}{m_p}\frac{\mathrm{d}m_p}{\mathrm{d}t}=\frac{\left[p_\infty - p_s(T_\infty)\right]}{\tau_t p_s(T_\infty)}\left[\mathrm{s}^{-1}\right]$$

- Thus defining a thermal relaxation time

$$\tau_t=\frac{\rho_p r_p^2 L^2 w_v}{3\kappa R T_\infty^2}\left[\mathrm{s}\right]$$

- Fluid and particles two-way coupled through fluid-temperature dependent particle relaxation model
- Change in particle velocity in the LPT is calculated according to the temperature-dependent dynamic viscosity, hence affecting the agglomeration rate and particle size distribution
- Rate of change of fluid condensed phase fraction determined according to particle-size and temperature-dependent thermal relaxation time

7. Methodology

UNIVERSITY OF LEEDS

Coefficient	Jones and Musonge [6]	Dianat et al. [8]
$C_{\varepsilon 1}$	1.4	1.44
$C_{\varepsilon 2}$	1.9	1.9
C_s	0.22	0.18333
C_t	0.18	0.18
C_d	0.18	0.18
C_e	0.18	0.15
C_1	1.5	3.0
C_2	-0.53	-0.44
C_3	0.67	0.46
C_4	-0.12	-0.23
C_5	0.0	0.0
C_6	$-3C_2/2 - C_3$	$-3C_2/2 - C_3$
C_7	$-2(C_4 + C_5)/3$	$-2(C_4 + C_5)/3$

- Second-moment Reynolds stress turbulence model with transport model coefficients show here
- Simulations performed in axisymmetric geometry
- Length (and time) scaled by the
- release nozzle diameter, *d*
- Domain: 0 to 40 *d* radially in *r*,
- 0 to 120 *d* axially in *z*
- Coarse grid: 80 x 240 cells, with 5 levels of AMR, equivalent to a maximum grid resolution of 1280 x 3840, totalling 4.9 million cells
- Inflow of CO_2 in the region z=0, r<0.5 at 2.1 MPa, 255 K, 100% CO2, 77% liquid phase, v_z = 65 m/s
- Particles: radius of 10^{-6} m, at 200 m/s with uniform density 1500 kg m^{-3}
- Simulations shown next are steady state with the maximum grid resolution through the AMR enabled

8. Results

UNIVERSITY OF LEEDS

- Preliminary simulations coupling fluid and particle model as above
- Compared to an uncoupled equilibrium simulation (shown in c), coupling considerably alters the physical conditions in the initial expansion (a and b)
- Temperatures are only as cold on the centreline
- Deviations from equilibrium model post-shock are entirely due to coupling of fluid and particles

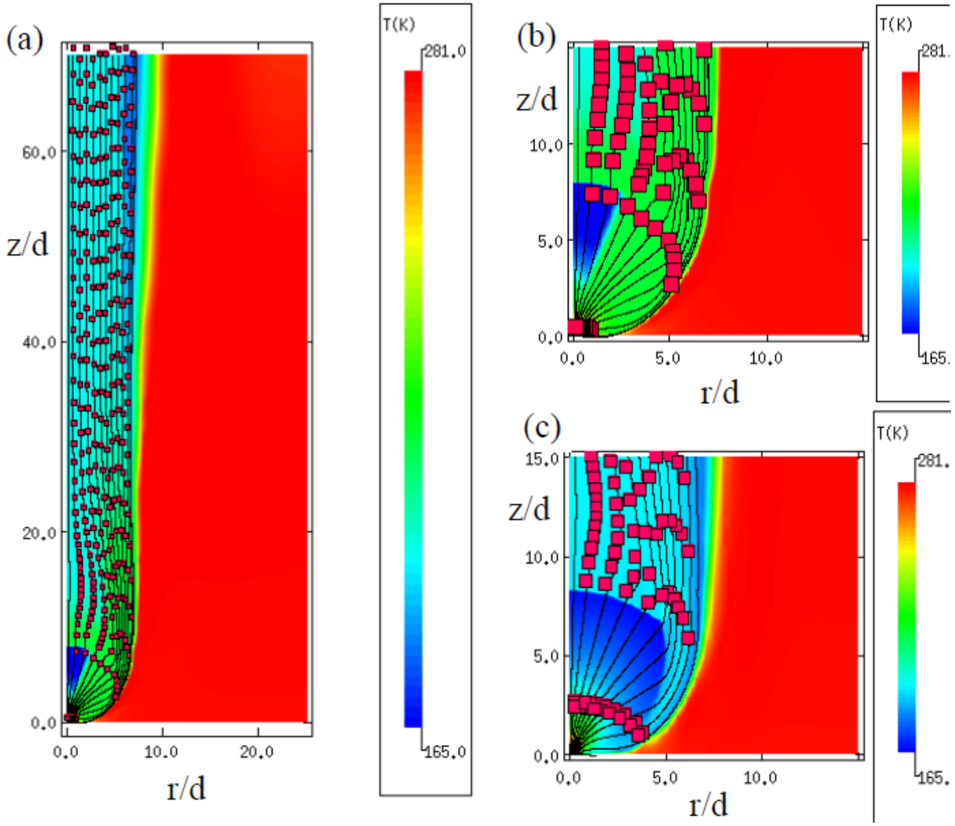

- Radially outer edges of the jet are considerably warmer: result of the delayed effect of the condensed phase through the dynamic and thermal relaxation occurring here
- By 50d, conditions back in agreement with equilibrium prediction, as observed

9. Conclusions and Further Work

UNIVERSITY OF LEEDS

- Mathematical models enable representative predictions of turbulent high pressure sonic CO_2 jets out of equilibrium
- Predictions validated against experimental data throughout
- Appropriate turbulent shear agglomeration model required to account for observed agglomeration
- High fidelity turbulence model with refinements for sonic jets required

- Applicable to RESS cleaning processes, CCS risk analysis and fracking processes

- Further work will investigate:
  - Supercritical releases with impurities
  - More complete particle evolution models
  - Extended turbulence models
  - Detailed application to industrial processes

Acknowledgements

UNIVERSITY OF LEEDS

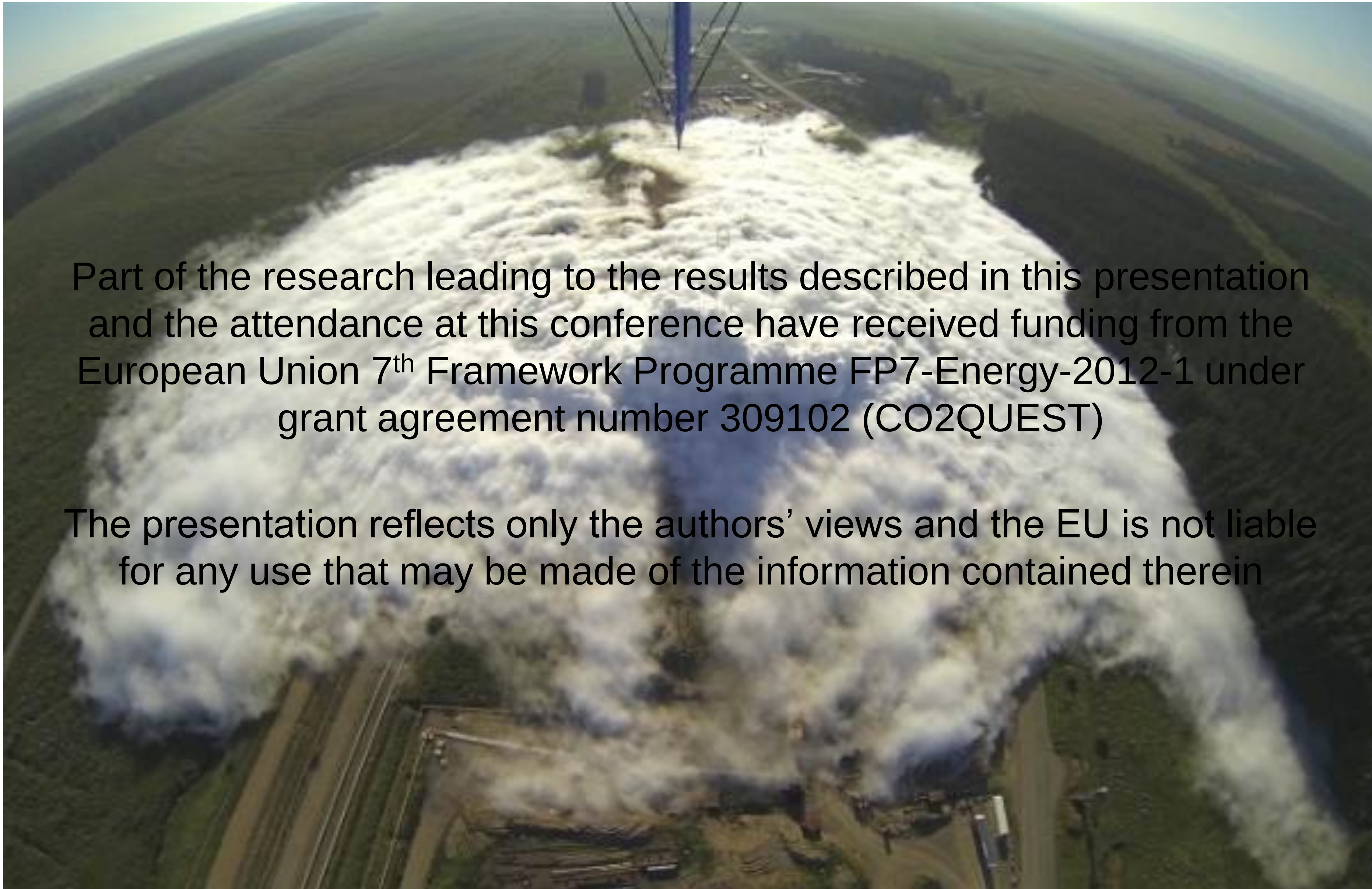

Part of the research leading to the results described in this presentation and the attendance at this conference have received funding from the European Union 7th Framework Programme FP7-Energy-2012-1 under grant agreement number 309102 (CO2QUEST)

The presentation reflects only the authors' views and the EU is not liable for any use that may be made of the information contained therein